Chapter 7

Kinematics of Closed Chains

Any kinematic chain that contains one or more loops is called a **closed chain**. Several examples of closed chains were encountered in Chapter 2, from the planar four-bar linkage to spatial mechanisms like the Stewart–Gough platform and the Delta robot (Figure 7.1). These mechanisms are examples of **parallel mechanisms**: closed chains consisting of fixed and moving platforms connected by a set of "legs." The legs themselves are typically open chains but sometimes can also be other closed chains (like the Delta robot in Figure 7.1(b)). In this chapter we analyze the kinematics of closed chains, paying special attention to parallel mechanisms.

The Stewart–Gough platform is used widely as both a motion simulator and a six-axis force–torque sensor. When used as a force–torque sensor, the six prismatic joints experience internal linear forces whenever any external force is applied to the moving platform; by measuring these internal linear forces one can estimate the applied external force. The Delta robot is a three-dof mechanism whose moving platform moves in such a way that it always remains parallel to the fixed platform. Because the three actuators are all attached to the three revolute joints of the fixed platform, the moving parts are relatively light; this allows the Delta to achieve very fast motions.

Closed chains admit a much greater variety of designs than open chains, and their kinematic and static analysis is consequently more complicated. This complexity can be traced to two defining features of closed chains: (i) not all joints are actuated, and (ii) the joint variables must satisfy a number of loop-closure constraint equations, which may or may not be independent depending on the

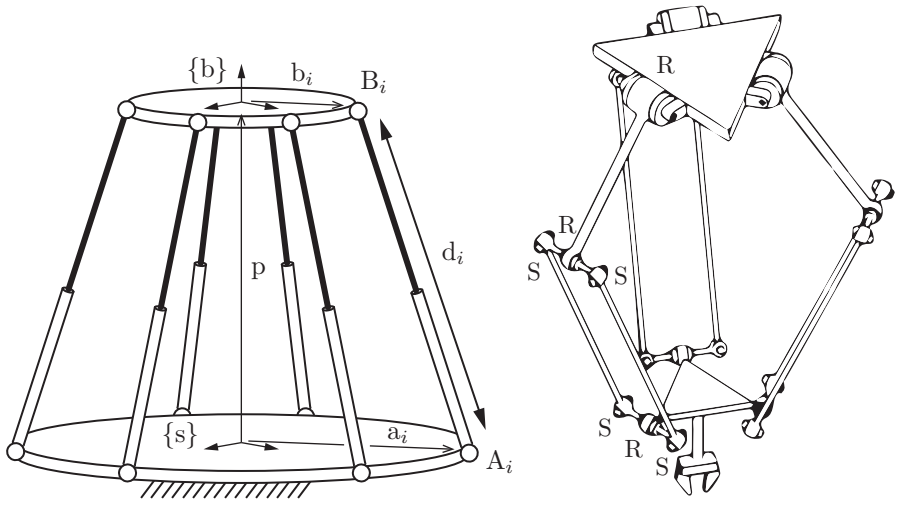

(a) Stewart–Gough platform. (b) Delta robot.

Figure 7.1: Two popular parallel mechanisms.

configuration of the mechanism. The presence of unactuated (or passive) joints, together with the fact that the number of actuated joints may deliberately be designed to exceed the mechanism's kinematic degrees of freedom – such mechanisms are said to be **redundantly actuated** – not only makes the kinematics analysis more challenging but also introduces new types of singularities not present in open chains.

Recall also that, for open chains, the kinematic analysis proceeds in a more or less straightforward fashion, with the formulation of the forward kinematics (e.g., via the product of exponentials formalism) followed by that of the inverse kinematics. For general closed chains it is usually difficult to obtain an explicit set of equations for the forward kinematics in the form $X = T(\theta)$, where $X \in SE(3)$ is the end-effector frame and $\theta \in \mathbb{R}^n$ are the joint coordinates. The more effective approaches exploit, as much as possible, any kinematic symmetries and other special features of the mechanism.

In this chapter we begin with a series of case studies involving some well-known parallel mechanisms and eventually build up a repertoire of kinematic analysis tools and methodologies for handling more general closed chains. Our focus will be on parallel mechanisms that are exactly actuated, i.e., the number of actuated degrees of freedom is equal to the number of degrees of freedom

of the mechanism. Methods for the forward and inverse position kinematics of parallel mechanisms are discussed; this is followed by the characterization and derivation of the constraint Jacobian, and the Jacobians of both the inverse and forward kinematics. The chapter concludes with a discussion of the different types of kinematic singularities that arise in closed chains.

7.1 Inverse and Forward Kinematics

One general observation that can be made for serial mechanisms versus parallel mechanisms is the following: for serial chains, the forward kinematics is generally straightforward while inverse kinematics may be complex (e.g., there may be multiple solutions or no solution). For parallel mechanisms, the inverse kinematics is often relatively straightforward (e.g., given the configuration of a platform, it may not be hard to determine the joint variables), while the forward kinematics may be quite complex: an arbitrarily chosen set of joint valuees may be infeasible or it may correspond to multiple possible configurations of the platform.

We now continue with two case studies, the 3×RPR planar parallel mechanism and its spatial counterpart, the 3×SPS Stewart–Gough platform. The analysis of these two mechanisms draws upon some simplification techniques that result in a reduced form of the governing kinematic equations, which in turn can be applied to the analysis of more general parallel mechanisms.

7.1.1 3×RPR Planar Parallel Mechanism

The first example we consider is the 3-dof planar 3×RPR parallel mechanism shown in Figure 7.2. A fixed frame {s} and body frame {b} are assigned to the platform as shown. The three prismatic joints are typically actuated while the six revolute joints are passive. Denote the lengths of each of the three legs by s_i, $i = 1, 2, 3$. The forward kinematics problem is to determine, for given values of $s = (s_1, s_2, s_3)$, the body frame's position and orientation. Conversely, the inverse kinematics problem is to determine s from $T_{sb} \in SE(2)$.

Let p be the vector from the origin of the {s} frame to the origin of the {b} frame. Let ϕ denote the angle measured from the $\hat{\mathrm{x}}_s$-axis of the {s} frame to the $\hat{\mathrm{x}}_b$-axis of the {b} frame. Further, define the vectors a_i, b_i, d_i, $i = 1, 2, 3$, as shown in the figure. From these definitions, clearly

$$\mathrm{d}_i = \mathrm{p} + \mathrm{b}_i - \mathrm{a}_i, \tag{7.1}$$

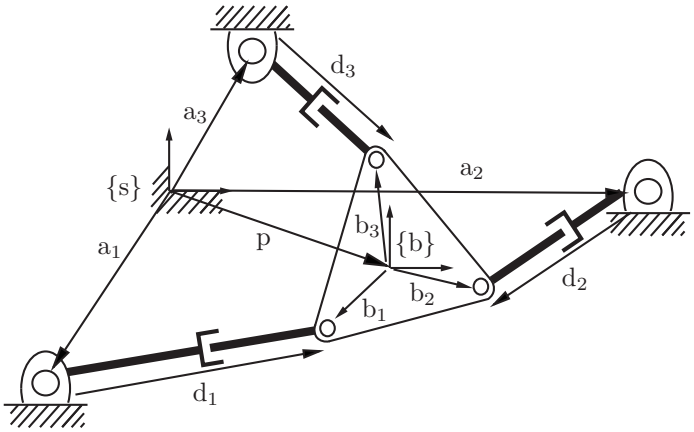

Figure 7.2: 3×RPR planar parallel mechanism.

for $i = 1, 2, 3$. Let

$$\begin{aligned}
\begin{bmatrix} p_x \\ p_y \end{bmatrix} &= \text{p in \{s\}-frame coordinates,} \\
\begin{bmatrix} a_{ix} \\ a_{iy} \end{bmatrix} &= \text{a}_i \text{ in \{s\}-frame coordinates,} \\
\begin{bmatrix} d_{ix} \\ d_{iy} \end{bmatrix} &= \text{d}_i \text{ in \{s\}-frame coordinates,} \\
\begin{bmatrix} b_{ix} \\ b_{iy} \end{bmatrix} &= \text{b}_i \text{ in \{b\}-frame coordinates.}
\end{aligned}$$

Note that (a_{ix}, a_{iy}) and (b_{ix}, b_{iy}) for $i = 1, 2, 3$ are all constant, and that, with the exception of the (b_{ix}, b_{iy}), all other vectors are expressed in {s}-frame coordinates. To express Equation (7.1) in terms of {s}-frame coordinates, b_i must be expressed in {s}-frame coordinates. This is straightforward: defining

$$R_{sb} = \begin{bmatrix} \cos\phi & -\sin\phi \\ \sin\phi & \cos\phi \end{bmatrix},$$

it follows that

$$\begin{bmatrix} d_{ix} \\ d_{iy} \end{bmatrix} = \begin{bmatrix} p_x \\ p_y \end{bmatrix} + R_{sb} \begin{bmatrix} b_{ix} \\ b_{iy} \end{bmatrix} - \begin{bmatrix} a_{ix} \\ a_{iy} \end{bmatrix},$$

for $i = 1, 2, 3$. Also, since $s_i^2 = d_{ix}^2 + d_{iy}^2$, we have

$$\begin{aligned} s_i^2 &= (p_x + b_{ix}\cos\phi - b_{iy}\sin\phi - a_{ix})^2 \\ &\quad + (p_y + b_{ix}\sin\phi + b_{iy}\cos\phi - a_{iy})^2, \end{aligned} \tag{7.2}$$

for $i = 1, 2, 3$.

Formulated as above, the inverse kinematics is trivial to compute: given values for (p_x, p_y, ϕ), the leg lengths (s_1, s_2, s_3) can be directly calculated from the above equations (negative values of s_i will not be physically realizable in most cases and can be ignored). In contrast, the forward kinematics problem of determining the body frame's position and orientation (p_x, p_y, ϕ) from the leg lengths (s_1, s_2, s_3) is not trivial. The following tangent half-angle substitution transforms the three equations in (7.2) into a system of polynomials in t, where

$$\begin{aligned} t &= \tan\frac{\phi}{2}, \\ \sin\phi &= \frac{2t}{1+t^2}, \\ \cos\phi &= \frac{1-t^2}{1+t^2}. \end{aligned}$$

After some algebraic manipulation, the system of polynomials (7.2) can eventually be reduced to a single sixth-order polynomial in t; this effectively shows that the 3×RPR mechanism may have up to six forward kinematics solutions. Showing that all six mathematical solutions are physically realizable requires further verification.

Figure 7.3(a) shows the mechanism at a singular configuration, where each leg length is identical and as short as possible. This configuration is a singularity, because extending the legs from this symmetric configuration causes the platform to rotate either clockwise or counterclockwise; we cannot predict which.[1] Singularities are covered in greater detail in Section 7.3. Figure 7.3(b) shows two solutions to the forward kinematics when all leg lengths are identical.

7.1.2 Stewart–Gough Platform

We now examine the inverse and forward kinematics of the 6×SPS Stewart–Gough platform of Figure 7.1(a). In this design the fixed and moving platforms are connected by six serial SPS structures, with the spherical joints passive and the prismatic joints actuated. The derivation of the kinematic equations is

[1] A third possibility is that the extending legs crush the platform!

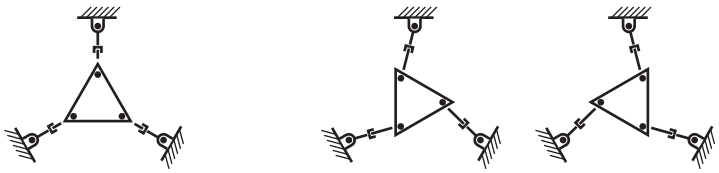

Figure 7.3: (a) The 3×RPR at a singular configuration. From this configuration, extending the legs may cause the platform to snap to a counterclockwise rotation or a clockwise rotation. (b) Two solutions to the forward kinematics when all prismatic joint extensions are identical.

close to that for the 3×RPR planar mechanism discussed above. Let {s} and {b} denote the fixed and body frames, respectively, and let d_i be the vector directed from joint A_i to joint B_i, $i = 1, \ldots, 6$. Referring to Figure 7.1(a), we make the following definitions:

$$
\begin{aligned}
&p \in \mathbb{R}^3 = \mathrm{p} \text{ in } \{\mathrm{s}\}\text{-frame coordinates},\\
&a_i \in \mathbb{R}^3 = \mathrm{a}_i \text{ in } \{\mathrm{s}\}\text{-frame coordinates},\\
&b_i \in \mathbb{R}^3 = \mathrm{b}_i \text{ in } \{\mathrm{b}\}\text{-frame coordinates},\\
&d_i \in \mathbb{R}^3 = \mathrm{d}_i \text{ in } \{\mathrm{s}\}\text{-frame coordinates},\\
&R \in SO(3) \text{ is the orientation of } \{\mathrm{b}\} \text{ as seen from } \{\mathrm{s}\}.
\end{aligned}
$$

In order to derive the kinematic constraint equations, note that, vectorially,

$$\mathrm{d}_i = \mathrm{p} + \mathrm{b}_i - \mathrm{a}_i, \qquad i = 1, \ldots, 6.$$

Writing the above equations explicitly in {s}-frame coordinates yields

$$d_i = p + Rb_i - a_i, \qquad i = 1, \ldots, 6.$$

Denoting the length of leg i by s_i, we have

$$s_i^2 = d_i^{\mathrm{T}} d_i = (p + Rb_i - a_i)^{\mathrm{T}}(p + Rb_i - a_i),$$

for $i = 1, \ldots, 6$. Note that a_i and b_i are all known constant vectors. Writing the constraint equations in this form, the inverse kinematics becomes straightforward: given p and R, the six leg lengths s_i can be determined directly from the above equations.

The forward kinematics is not as straightforward: given each leg length s_i, $i = 1, \ldots, 6$, we must solve for $p \in \mathbb{R}^3$ and $R \in SO(3)$. These six constraint equations, together with six further constraints imposed by the condition $R^{\mathrm{T}}R = I$, constitute a set of 12 equations in 12 unknowns (three for p, nine for R).

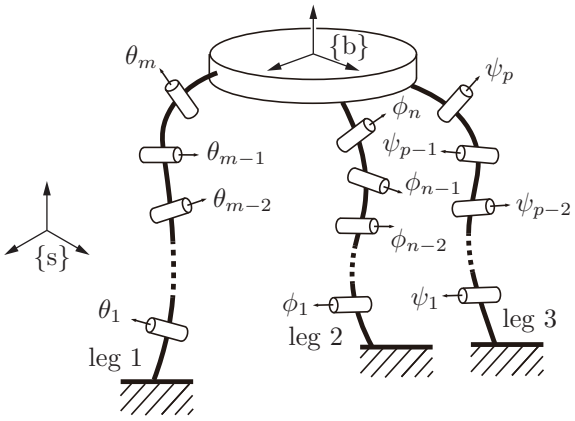

Figure 7.4: A general parallel mechanism.

7.1.3 General Parallel Mechanisms

For both the 3×RPR mechanism and the Stewart–Gough platform, we were able to exploit certain features of the mechanism that resulted in a reduced set of equations; for example, the fact that the legs of the Stewart–Gough platform can be modeled as straight lines considerably simplified the analysis. In this section we briefly consider the case when the legs are general open chains.

Consider such a parallel mechanism, as shown in Figure 7.4; here the fixed and moving platforms are connected by three open chains. Let the configuration of the moving platform be given by T_{sb}. Denote the forward kinematics of the three chains by $T_1(\theta)$, $T_2(\phi)$, and $T_3(\psi)$, respectively, where $\theta \in \mathbb{R}^m$, $\phi \in \mathbb{R}^n$, and $\psi \in \mathbb{R}^p$. The loop-closure conditions can be written $T_{sb} = T_1(\theta) = T_2(\phi) = T_3(\psi)$. Eliminating T_{sb}, we get

$$T_1(\theta) = T_2(\phi), \tag{7.3}$$
$$T_2(\phi) = T_3(\psi). \tag{7.4}$$

Equations (7.3) and (7.4) each consist of 12 equations (nine for the rotation component and three for the position component), six of which are independent: from the rotation matrix constraint $R^{\mathrm{T}}R = I$, the nine equations for the rotation component can be reduced to a set of three independent equations. Thus there are 24 constraint equations, 12 of which are independent, with $n+m+p$ unknown variables. The mechanism therefore has $d = n + m + p - 12$ degrees of freedom.

In the forward kinematics problem, given d values for the joint variables (θ, ϕ, ψ), Equations (7.3) and (7.4) can be solved for the remaining joint vari-

ables. Generally this is not trivial and multiple solutions are likely. Once the joint values for any one of the open chain legs are known, the forward kinematics of that leg can then be evaluated to determine the forward kinematics of the closed chain.

In the inverse kinematics problem, given the body-frame displacement $T_{sb} \in SE(3)$, we set $T = T_1 = T_2 = T_3$ and solve Equations (7.3) and (7.4) for the joint variables (θ, ϕ, ψ). As suggested by these case studies, for most parallel mechanisms there are features of the mechanism that can be exploited to eliminate some of these equations and simplify them to a more computationally amenable form.

7.2 Differential Kinematics

We now consider the differential kinematics of parallel mechanisms. Unlike the case for open chains, in which the objective is to relate the input joint velocities to the twist of the end-effector frame, the analysis for closed chains is complicated by the fact that not all the joints are actuated. Only the actuated joints can be prescribed input velocities; the velocities of the remaining passive joints must then be determined from the kinematic constraint equations. These passive joint velocities are usually required in order to eventually determine the twist of the closed chain's end-effector frame.

For open chains, the Jacobian of the forward kinematics is central to the velocity and static analysis. For closed chains, in addition to the forward kinematics Jacobian, the Jacobian defined by the kinematic constraint equations – we will call this the **constraint Jacobian** – also plays a central role in the velocity and static analysis. Usually there are features of the mechanism that can be exploited to simplify and reduce the procedure for obtaining the two Jacobians. We illustrate this with a case study of the Stewart–Gough platform, and show that the Jacobian of the inverse kinematics can be obtained straightforwardly via static analysis. The velocity analysis for more general parallel mechanisms is then detailed.

7.2.1 Stewart–Gough Platform

Earlier we saw that the inverse kinematics for the Stewart–Gough platform can be solved analytically. That is, given the body-frame orientation $R \in SO(3)$ and position $p \in \mathbb{R}^3$, the leg lengths $s \in \mathbb{R}^6$ can be obtained analytically in the functional form $s = g(R, p)$. In principle one could differentiate this equation

and manipulate it into the form

$$\dot{s} = G(R,p)\mathcal{V}_s, \tag{7.5}$$

where $\dot{s} \in \mathbb{R}^6$ denotes the leg velocities, $\mathcal{V}_s \in \mathbb{R}^6$ is the spatial twist, and $G(R,p) \in \mathbb{R}^{6\times 6}$ is the Jacobian of the inverse kinematics. In most cases this procedure will require considerable algebraic manipulation.

Here we take a different approach, based on the conservation of power principle used to determine the static relationship $\tau = J^{\mathrm{T}}\mathcal{F}$ for open chains. The static relationship for closed chains can be expressed in exactly the same form. We illustrate this with an analysis of the Stewart–Gough platform.

In the absence of external forces, the only forces applied to the moving platform occur at the spherical joints. In what follows, all vectors are expressed in {s}-frame coordinates. Let

$$f_i = \hat{n}_i \tau_i$$

be the three-dimensional linear force applied by leg i, where $\hat{n}_i \in \mathbb{R}^3$ is a unit vector indicating the direction of the applied force and $\tau_i \in \mathbb{R}$ is the magnitude of the linear force. The moment m_i generated by f_i is

$$m_i = r_i \times f_i,$$

where $r_i \in \mathbb{R}^3$ denotes the vector from the {s}-frame origin to the point of application of the force (the location of spherical joint i in this case). Since neither the spherical joint at the moving platform nor the spherical joint at the fixed platform can resist any torques about them, the force f_i must be along the line of the leg. Therefore, instead of calculating the moment m_i using the spherical joint at the moving platform, we can calculate the moment using the spherical joint at the fixed platform:

$$m_i = q_i \times f_i,$$

where $q_i \in \mathbb{R}^3$ denotes the vector from the fixed-frame origin to the base joint of leg i. Since q_i is constant, expressing the moment as $q_i \times f_i$ is preferable.

Combining f_i and m_i into the six-dimensional wrench $\mathcal{F}_i = (m_i, f_i)$, the resultant wrench $\mathcal{F}_s$ on the moving platform is given by

$$\begin{aligned}
\mathcal{F}_s &= \sum_{i=1}^{6} \mathcal{F}_i = \sum_{i=1}^{6} \begin{bmatrix} r_i \times \hat{n}_i \\ \hat{n}_i \end{bmatrix} \tau_i \\
&= \begin{bmatrix} -\hat{n}_1 \times q_1 & \cdots & -\hat{n}_6 \times q_6 \\ \hat{n}_1 & \cdots & \hat{n}_6 \end{bmatrix} \begin{bmatrix} \tau_1 \\ \vdots \\ \tau_6 \end{bmatrix} \\
&= J_s^{-T}\tau,
\end{aligned}$$

where J_s is the spatial Jacobian of the forward kinematics, with inverse given by

$$J_s^{-1} = \begin{bmatrix} -\hat{n}_1 \times q_1 & \cdots & -\hat{n}_6 \times q_6 \\ \hat{n}_1 & \cdots & \hat{n}_6 \end{bmatrix}^{\mathrm{T}}.$$

7.2.2 General Parallel Mechanisms

Because of its kinematic structure, the Stewart–Gough platform lends itself particularly well to a static analysis, as each of the six joint forces are directed along their respective legs. The Jacobian (or more precisely, the inverse Jacobian) can therefore be derived in terms of the screws associated with each straight-line leg. In this subsection we consider more general parallel mechanisms where the static analysis is less straightforward. Using the previous three-legged spatial parallel mechanism of Figure 7.4 as an illustrative example, we derive a procedure for determining the forward kinematics Jacobian that can be generalized to other types of parallel mechanisms.

The mechanism of Figure 7.4 consists of two platforms connected by three legs with m, n, and p joints, respectively. For simplicity, we will take $m = n = p = 5$, so that the mechanism has $d = n + m + p - 12 = 3$ degrees of freedom (generalizing what follows to different types and numbers of legs is completely straightforward). For the fixed and body frames indicated in the figure, we can write the forward kinematics for the three chains as follows:

$$\begin{aligned} T_1(\theta_1, \theta_2, \ldots, \theta_5) &= e^{[S_1]\theta_1} e^{[S_2]\theta_2} \cdots e^{[S_5]\theta_5} M_1, \\ T_2(\phi_1, \phi_2, \ldots, \phi_5) &= e^{[P_1]\phi_1} e^{[P_2]\phi_2} \cdots e^{[P_5]\phi_5} M_2, \\ T_3(\psi_1, \psi_2, \ldots, \psi_5) &= e^{[Q_1]\psi_1} e^{[Q_2]\psi_2} \cdots e^{[Q_5]\psi_5} M_3. \end{aligned}$$

The kinematic loop constraints can be expressed as

$$T_1(\theta) = T_2(\phi), \tag{7.6}$$
$$T_2(\phi) = T_3(\psi). \tag{7.7}$$

Since these constraints must be satisfied at all times, we can express their time derivatives in terms of their spatial twists, using

$$\dot{T}_1 T_1^{-1} = \dot{T}_2 T_2^{-1}, \tag{7.8}$$
$$\dot{T}_2 T_2^{-1} = \dot{T}_3 T_3^{-1}. \tag{7.9}$$

Since $\dot{T}_i T_i^{-1} = [\mathcal{V}_i]$, where $\mathcal{V}_i$ is the spatial twist of chain i's end-effector frame, the above identities can also be expressed in terms of the forward kinematics

Jacobian for each chain:

$$J_1(\theta)\dot{\theta} = J_2(\phi)\dot{\phi}, \tag{7.10}$$
$$J_2(\phi)\dot{\phi} = J_3(\psi)\dot{\psi}, \tag{7.11}$$

which can be rearranged as

$$\begin{bmatrix} J_1(\theta) & -J_2(\phi) & 0 \\ 0 & -J_2(\phi) & J_3(\psi) \end{bmatrix} \begin{bmatrix} \dot{\theta} \\ \dot{\phi} \\ \dot{\psi} \end{bmatrix} = 0. \tag{7.12}$$

Now we rearrange the 15 joints into those that are actuated and those that are passive. Assume without loss of generality that the three actuated joints are $(\theta_1, \phi_1, \psi_1)$. Define the vector of the actuated joints $q_a \in \mathbb{R}^3$ and the vector of the passive joints $q_p \in \mathbb{R}^{12}$ as

$$q_a = \begin{bmatrix} \theta_1 \\ \phi_1 \\ \psi_1 \end{bmatrix}, \qquad q_p = \begin{bmatrix} \theta_2 \\ \vdots \\ \phi_5 \end{bmatrix},$$

and we have $q = (q_a, q_p) \in \mathbb{R}^{15}$. Equation (7.12) can now be rearranged into the form

$$\begin{bmatrix} H_a(q) & H_p(q) \end{bmatrix} \begin{bmatrix} \dot{q}_a \\ \dot{q}_p \end{bmatrix} = 0, \tag{7.13}$$

or, equivalently,

$$H_a\dot{q}_a + H_p\dot{q}_p = 0, \tag{7.14}$$

where $H_a \in \mathbb{R}^{12\times 3}$ and $H_p \in \mathbb{R}^{12\times 12}$. If H_p is invertible, we have

$$\dot{q}_p = -H_p^{-1}H_a\dot{q}_a. \tag{7.15}$$

So, assuming that H_p is invertible, once the velocities of the actuated joints are given, then the velocities of the remaining passive joints can be obtained uniquely via Equation (7.15).

It still remains to derive the forward kinematics Jacobian with respect to the actuated joints, i.e., to find $J_a(q) \in \mathbb{R}^{6\times 3}$ satisfying $\mathcal{V}_s = J_a(q)\dot{q}_a$, where $\mathcal{V}_s$ is the spatial twist of the end-effector frame. For this purpose we can use the forward kinematics for any of the three open chains: for example, in terms of chain 1, $J_1(\theta)\dot{\theta} = \mathcal{V}_s$, and from Equation (7.15) we can write

$$\dot{\theta}_2 = g_2^{\mathrm{T}}\dot{q}_a, \tag{7.16}$$
$$\dot{\theta}_3 = g_3^{\mathrm{T}}\dot{q}_a, \tag{7.17}$$
$$\dot{\theta}_4 = g_4^{\mathrm{T}}\dot{q}_a, \tag{7.18}$$
$$\dot{\theta}_5 = g_5^{\mathrm{T}}\dot{q}_a, \tag{7.19}$$

where each $g_i(q) \in \mathbb{R}^3$, for $i = 2, \ldots, 5$, can be obtained from Equation (7.15). Defining the row vector $e_1^{\mathrm{T}} = [1\ 0\ 0]$, the differential forward kinematics for chain 1 can now be written

$$\mathcal{V}_s = J_1(\theta) \begin{bmatrix} e_1^{\mathrm{T}} \\ g_2^{\mathrm{T}} \\ g_3^{\mathrm{T}} \\ g_4^{\mathrm{T}} \\ g_5^{\mathrm{T}} \end{bmatrix} \begin{bmatrix} \dot{\theta}_1 \\ \dot{\phi}_1 \\ \dot{\psi}_1 \end{bmatrix}. \tag{7.20}$$

Since we are seeking $J_a(q)$ in $\mathcal{V}_s = J_a(q)\dot{q}_a$, and since $\dot{q}_a^{\mathrm{T}} = [\dot{\theta}_1\ \dot{\phi}_1\ \dot{\psi}_1]$, from the above it now follows that

$$J_a(q) = J_1(q_1, \ldots, q_5) \begin{bmatrix} e_1^{\mathrm{T}} \\ g_2(q)^{\mathrm{T}} \\ g_3(q)^{\mathrm{T}} \\ g_4(q)^{\mathrm{T}} \\ g_5(q)^{\mathrm{T}} \end{bmatrix}; \tag{7.21}$$

this equation could also have been derived using either chain 2 or chain 3.

Given values for the actuated joints q_a, we still need to solve for the passive joints q_p from the loop-constraint equations. Eliminating in advance as many elements of q_p as possible will obviously simplify matters. The second point to note is that $H_p(q)$ may become singular, in which case $\dot{q}_p$ cannot be obtained from $\dot{q}_a$. Configurations in which $H_p(q)$ becomes singular correspond to **actuator singularities**, which are discussed in the next section.

7.3 Singularities

Characterizing the singularities of closed chains involves many more subtleties than for open chains. In this section we highlight the essential features of closed-chain singularities via two planar examples: a four-bar linkage (see Figure 7.5) and a five-bar linkage (see Figure 7.6). On the basis of these examples we classify closed-chain singularities into three basic types: **actuator singularities**, **configuration space singularities**, and **end-effector singularities**.

We begin with the four-bar linkage of Figure 7.5. Recall from Chapter 2 that its C-space is a one-dimensional curve embedded in a four-dimensional ambient space (each dimension is parametrized by one of the four joints). Projecting the C-space onto the joint angles (θ, ϕ) leads to the bold curve shown in Figure 7.5.

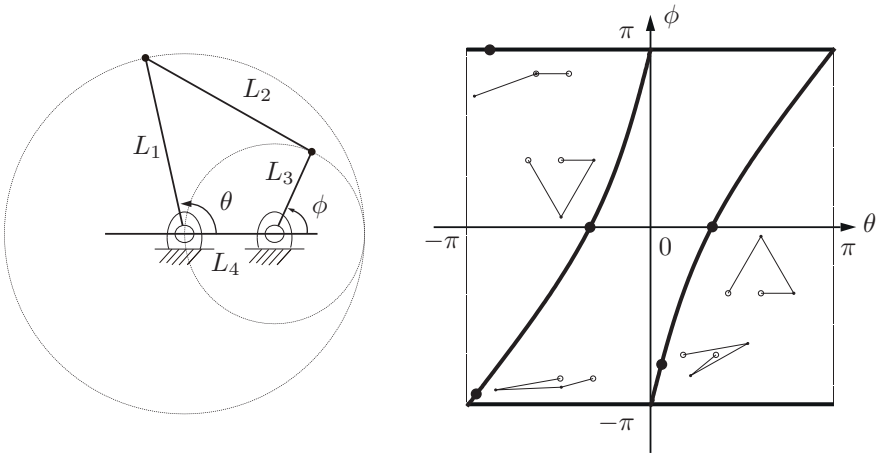

Figure 7.5: (Left) A planar four-bar linkage and (right) its one-dimensional C-space, represented in bold in the θ–ϕ space. Also shown on the right are five sample configurations (bold dots), three of which are near bifurcation points and two of which are far removed from a bifurcation point.

In terms of θ and ϕ, the kinematic loop constraint equations for the four-bar linkage can be expressed as

$$\phi = \tan^{-1}\left(\frac{\beta}{\alpha}\right) \pm \cos^{-1}\left(\frac{\gamma}{\sqrt{\alpha^2+\beta^2}}\right), \tag{7.22}$$

where

$$\alpha = 2L_3L_4 - 2L_1L_3\cos\theta, \tag{7.23}$$
$$\beta = -2L_1L_3\sin\theta, \tag{7.24}$$
$$\gamma = L_2^2 - L_4^2 - L_3^2 - L_1^2 + 2L_1L_4\cos\theta. \tag{7.25}$$

The existence and uniqueness of solutions to the equations above depend on the link lengths $L_1, \ldots, L_4$. In particular, a solution will fail to exist if $\gamma^2 \leq \alpha^2+\beta^2$. Figure 7.5 depicts the feasible configurations for the choice of link lengths $L_1 = L_2 = 4$ and $L_3 = L_4 = 2$. For this set of link lengths, θ and ϕ both range from 0 to 2π.

A distinctive feature of Figure 7.5 is the presence of **bifurcation points** where branches of the curve meet. As the mechanism approaches these configurations, it has a choice of which branch to follow. Figure 7.5 shows sample

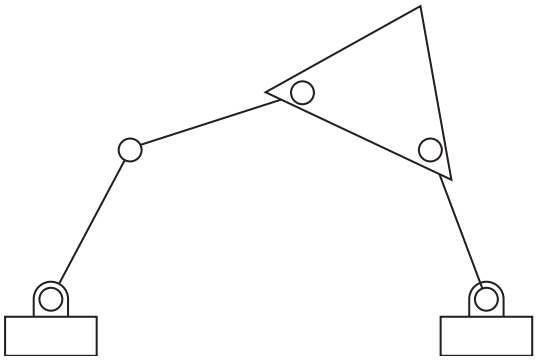

Figure 7.6: A planar five-bar linkage.

configurations on the different branches near, and also far from, the bifurcation points.

We now turn to the five-bar linkage of Figure 7.6. The kinematic loop-constraint equations can be written

$$L_1 \cos\theta_1 + \cdots + L_4 \cos(\theta_1 + \theta_2 + \theta_3 + \theta_4) = L_5, \tag{7.26}$$
$$L_1 \sin\theta_1 + \cdots + L_4 \sin(\theta_1 + \theta_2 + \theta_3 + \theta_4) = 0, \tag{7.27}$$

where we have eliminated in advance the joint variable θ_5 from the loop-closure conditions. Writing these two equations in the form $f(\theta_1, \ldots, \theta_4) = 0$, where $f : \mathbb{R}^4 \to \mathbb{R}^2$, the configuration space can be regarded as a two-dimensional surface in $\mathbb{R}^4$. Like the bifurcation points of the four-bar linkage, self-intersections of the surface can also occur. At such points the constraint Jacobian loses rank. For the five-bar linkage, any point θ at which

$$\operatorname{rank}\left(\frac{\partial f}{\partial \theta}(\theta)\right) < 2 \tag{7.28}$$

corresponds to what we call a **configuration space singularity**. Figure 7.7 illustrates the possible configuration space singularities of the five-bar linkage. Notice that so far we have made no mention of which joints of the five-bar linkage are actuated, or where the end-effector frame is placed. The notion of a configuration space singularity is completely independent of the choice of actuated joints or where the end-effector frame is placed.

We now consider the case when two joints of the five-bar linkage are actuated. Referring to Figure 7.8, the two revolute joints fixed to ground are the

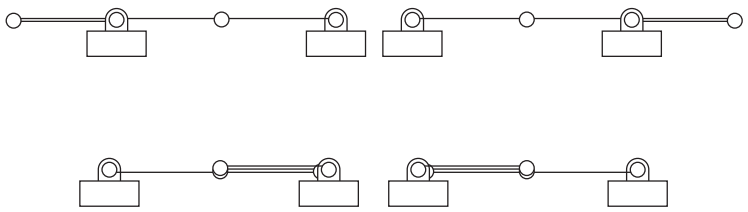

Figure 7.7: Configuration space singularities of the planar five-bar linkage.

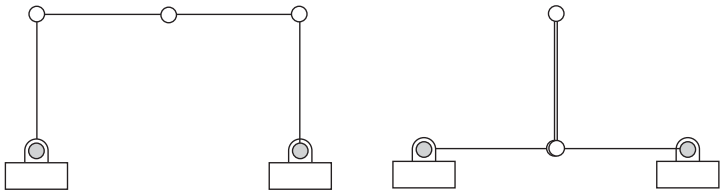

Figure 7.8: Actuator singularities of the planar five-bar linkage, where in each case the two actuated joints are shaded gray. The singularity on the left is nondegenerate, while the singularity on the right is degenerate.

.

actuated joints. Under normal operating conditions, the motions of the actuated joints can be independently controlled. Alternatively, locking the actuated joints should immobilize the five-bar linkage and turn it into a rigid structure.

For the **nondegenerate actuator singularity** shown in the left-hand panel of Figure 7.8, rotating the two actuated joints oppositely and outward will pull the mechanism apart; rotating them oppositely and inward would either crush the inner two links or cause the center joint to unpredictably buckle upward or downward. For the **degenerate actuator singularity** shown on the right, even when the actuated joints are locked in place the inner two links are free to rotate.

The reason for classifying these singularities as **actuator singularities** is

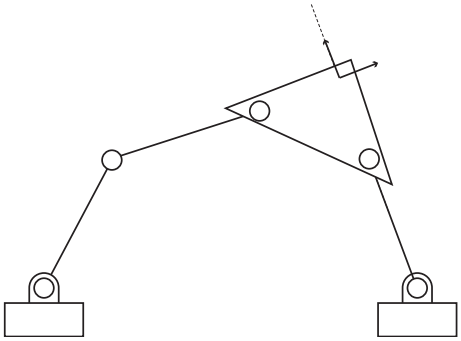

Figure 7.9: End-effector singularity of the planar five-bar linkage.

that, by relocating the actuators to a different set of joints, such singularities can be eliminated. For both the degenerate and nondegenerate actuator singularities of the five-bar linkage, relocating one actuator to one of the other three passive joints eliminates the singularity.

Visualizing the actuator singularities of the planar five-bar linkage is straightforward enough but, for more complex spatial closed chains, visualization may be difficult. Actuator singularities can be characterized mathematically by the rank of the constraint Jacobian. As before, write the kinematic loop constraints in differential form:

$$H(q)\dot{q} = \begin{bmatrix} H_a(q) & H_p(q) \end{bmatrix} \begin{bmatrix} \dot{q}_a \\ \dot{q}_p \end{bmatrix} = 0, \tag{7.29}$$

where $q_a \in \mathbb{R}^a$ is the vector of the a actuated joints and $q_p \in \mathbb{R}^p$ is the vector of the p passive joints. It follows that $H(q) \in \mathbb{R}^{p\times(a+p)}$ and that $H_p(q)$ is a $p \times p$ matrix.

With the above definitions, we have the following:

- If rank $H_p(q) < p$ then q is an **actuator singularity**. Distinguishing between **degenerate** and **nondegenerate** singularities involves additional mathematical subtleties and relies on second-order derivative information; we do not pursue this further here.

- If rank $H(q) < p$ then q is a **configuration space singularity**. Note that under this condition $H_p(q)$ is also singular (the converse is not true, however). The configuration space singularities can therefore be regarded as the intersection of all possible actuator singularities obtained over all possible combinations of actuated joints.

The final class of singularities depends on the choice of end-effector frame. For the five-bar linkage, let us ignore the orientation of the end-effector frame and focus exclusively on the x–y location of the end-effector frame. Figure 7.9 shows the five-bar linkage in an **end-effector singularity** for a given choice of end-effector location. Note that velocities along the dashed line are not possible in this configuration, similarly to the case of singularities for open chains. To see why these velocities are not possible, consider the effective 2R open chain created by the rightmost joint, the link connecting it to the platform, the joint on the platform, and the effective link connecting the platform joint to the end-effector frame. Since the two links of the 2R robot are aligned, the end-effector frame can have no component of motion along the direction of the links.

End-effector singularities are independent of the choice of actuated joints. They can be mathematically characterized as follows. Choose any valid set of actuated joints q_a such that the mechanism is not at an actuator singularity. Write the forward kinematics in the form

$$f(q_a) = T_{sb}. \tag{7.30}$$

One can then check for rank deficiencies in the Jacobian of f, as was done for open chains, to determine the presence of an end-effector singularity.

7.4 Summary

- Any kinematic chain that contains one or more loops is called a **closed chain**. **Parallel mechanisms** are a class of closed chains that are characterized by two platforms – one moving and one stationary – connected by several legs; the legs are typically open chains, but can themselves be closed chains. The kinematic analysis of closed chains is complicated compared with that of open chains because only a subset of joints is actuated and because the joint variables must satisfy a number of loop-closure constraint equations which may or may not be independent, depending on the configuration of the mechanism.
- For a parallel mechanism with equal numbers of actuators and degrees of freedom, the inverse kinematics problem involves finding, from the given position and orientation of the moving platform, the joint coordinates of the actuated joints. For well-known parallel mechanisms like the planar 3×RPR and the spatial Stewart–Gough platform, the inverse kinematics admits unique solutions.
- For a parallel mechanism with equal numbers of actuators and degrees of freedom, the forward kinematics problem involves finding the position and

orientation of the moving platform given coordinates for all the actuated joints. For well-known parallel mechanisms like the planar 3×RPR and the spatial Stewart–Gough platform, the forward kinematics usually admits multiple solutions. In the case of the most general Stewart–Gough platform, a maximum of 40 solutions is possible.

- The differential kinematics of a closed chain relates the velocities of the actuated joints to the linear and angular velocities of the moving platform's end-effector frame. For an m-dof closed chain consisting of n one-dof joints, let $q_a \in \mathbb{R}^m$ and $q_p \in \mathbb{R}^{n-m}$ respectively denote the vector of actuated and passive joints. The kinematic loop-closure constraints can then be expressed in differential form as $H_a\dot{q}_a + H_p\dot{q}_p = 0$, where $H_a \in \mathbb{R}^{(n-m)\times m}$ and $H_p \in \mathbb{R}^{(n-m)\times(n-m)}$ are configuration-dependent matrices. If H_p is invertible then $\dot{q}_p = -H_p^{-1}H_a\dot{q}_a$; the differential forward kinematics can then be expressed in the form $\mathcal{V} = J(q_a, q_p)\dot{q}_a$, where $\mathcal{V}$ is the twist of the end-effector frame and $J(q_a, q_p) \in \mathbb{R}^{6\times m}$ is a configuration-dependent Jacobian matrix. For closed chains like the Stewart–Gough platform, the differential forward kinematics can also be obtained from a static analysis by exploiting the fact that, just as for open chains, the wrench $\mathcal{F}$ applied by the end-effector is related to the joint forces or torques τ by $\tau = J^{\mathrm{T}}\mathcal{F}$.

- Singularities for closed chains can be classified into three types: (i) configuration space singularities at self-intersections of the configuration space surface (also called bifurcation points for one-dimensional configuration spaces); (ii) nondegenerate actuator singularities, when the actuated joints cannot be independently actuated, and degenerate actuator singularities when locking all joints fails to make the mechanism a rigid structure; and (iii) end-effector singularities when the end-effector loses one or more degrees of freedom of motion. Configuration space singularities are independent of the choice of actuated joints, while actuator singularities depend on which joints are actuated. End-effector singularities depend on the placement of the end-effector frame but do not depend on the choice of actuated joints.

7.5 Notes and References

A comprehensive reference for all aspects of parallel robots is [116]; [117] provides a more compact summary but with more recent references. One of the major outstanding problems in parallel mechanism kinematics in the 1990s was

the question of how many forward kinematics solutions can exist for the general 6–6 platform consisting of six SPS legs (with the prismatic joints actuated) connecting a fixed platform to a moving platform. Raghavan and Roth [143] showed that there can be at most 40 solutions, while Husty [62] developed an algorithm for finding all 40 solutions.

Singularities of closed chains have also received considerable attention in the literature. The terminology for closed-chain singularities used in this chapter was introduced in [136]; in particular, the distinction between degenerate and nondegenerate actuator singularities derives in part from similar terminology used in Morse theory to identify those critical points where the Hessian is singular (i.e., degenerate). The 3×UPU mechanism, which is addressed in the exercises in both Chapter 2 and the current chapter, can exhibit rather unusual singularity behavior; a more detailed singularity analysis of this mechanism can be found in [52, 35].

7.6 Exercises

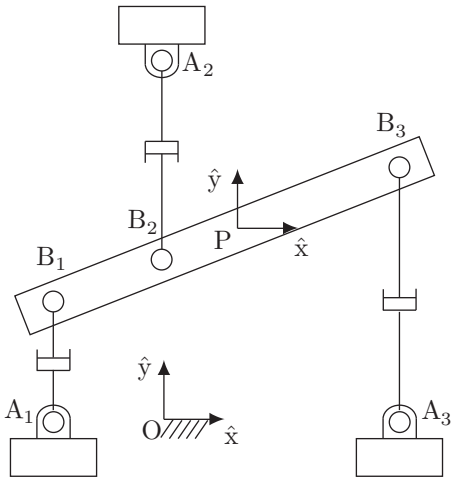

Figure 7.10: 3×RPR planar parallel mechanism.

Exercise 7.1 In the 3×RPR planar parallel mechanism of Figure 7.10 the prismatic joints are actuated. Define $a_i \in \mathbb{R}^2$ to be the vector from the fixed-

frame origin O to joint A_i, $i = 1, 2, 3$, expressed in fixed-frame coordinates. Define $b_i \in \mathbb{R}^2$ to be the vector from the moving-platform-frame origin P to joint B_i, $i = 1, 2, 3$, defined in terms of the moving-platform-frame coordinates.

(a) Solve the inverse kinematics.
(b) Derive a procedure to solve the forward kinematics.
(c) Is the configuration shown in the figure an end-effector singularity? Explain your answer by examining the inverse kinematics Jacobian. Is this also an actuator singularity?

Exercise 7.2 For the 3×RPR planar parallel mechanism in Figure 7.11(a), let ϕ be the angle measured from the {s}-frame $\hat{x}$-axis to the {b}-frame $\hat{x}$-axis, and $p \in \mathbb{R}^2$ be the vector from the {s}-frame origin to the {b}-frame origin, expressed in {s}-frame coordinates. Let $a_i \in \mathbb{R}^2$ be the vector from the {s}-frame origin to the three joints fixed to ground, $i = 1, 2, 3$ (note that two of the joints are overlapping), expressed in {s}-frame coordinates. Let $b_i \in \mathbb{R}^2$ be the vector from the {b}-frame origin to the three joints attached to the moving platform, $i = 1, 2, 3$ (note that two of the joints are overlapping), expressed in {b}-frame coordinates. The three prismatic joints are actuated, and the leg lengths are θ_1, θ_2, and θ_3, as shown.

(a) Derive a set of independent equations relating (ϕ, p) and $(\theta_1, \theta_2, \theta_3)$.
(b) What is the maximum possible number of forward kinematics solutions?
(c) Assuming static equilibrium, given joint forces $\tau = (1, 0, -1)$ applied at joints $(\theta_1, \theta_2, \theta_3)$, find the planar wrench (m_{bz}, f_{bx}, f_{by}) in the end-effector frame {b}.
(d) Now construct a mechanism with three connected 3×RPR parallel mechanisms as shown in Figure 7.11(b). How many degrees of freedom does this mechanism have?

Exercise 7.3 For the 3×RRR planar parallel mechanism shown in Figure 7.12, let ϕ be the orientation of the end-effector frame and $p \in \mathbb{R}^2$ be the vector p expressed in fixed-frame coordinates. Let $a_i \in \mathbb{R}^2$ be the vector a_i expressed in fixed-frame coordinates and $b_i \in \mathbb{R}^2$ be the vector b_i expressed in the moving body-frame coordinates.

(a) Derive a set of independent equations relating (ϕ, p) and $(\theta_1, \theta_2, \theta_3)$.
(b) What is the maximum possible number of inverse and forward kinematic solutions for this mechanism?

Exercise 7.4 Figure 7.13 shows a six-bar linkage in its zero position. Let (p_x, p_y) be the position of the {b}-frame origin expressed in {s}-frame coordinates,

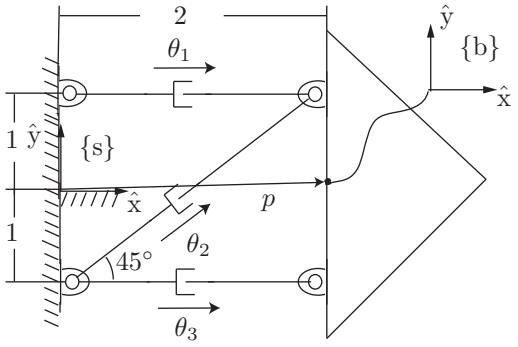

(a) 3×RPR planar parallel mechanism.

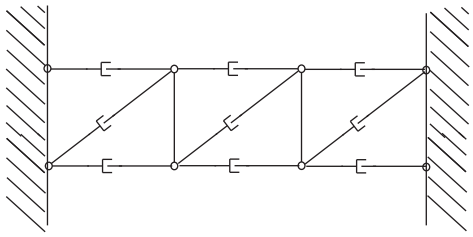

(b) Truss.

Figure 7.11: 3×RPR planar parallel mechanism and truss structure.

and let ϕ be the orientation of the {b} frame. The inverse kinematics problem is defined as that of finding the joint variables (θ, ψ) given (p_x, p_y, ϕ).

(a) In order to solve the inverse kinematics problem, how many equations are needed? Derive these equations.

(b) Assume that joints A, D, and E are actuated. Determine whether the configuration shown in Figure 7.13 is an actuator singularity by analyzing an equation of the form

$$\begin{bmatrix} H_a & H_p \end{bmatrix} \begin{bmatrix} \dot{q}_a \\ \dot{q}_p \end{bmatrix} = 0,$$

where q_a is the vector of the actuated joints and q_p is the vector of the passive joints.

(c) Suppose instead that joints A, B, and D are actuated. Find the forward kinematics Jacobian J_a from $\mathcal{V}_s = J_a \dot{q}_a$, where $\mathcal{V}_s$ is the twist in {s}-frame coordinates and $\dot{q}_a$ is the vector of actuated joint rates.

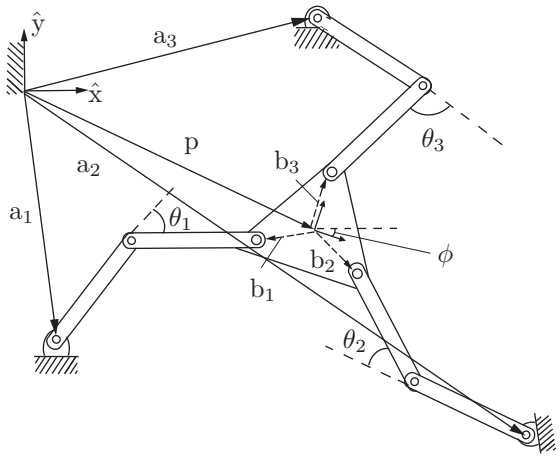

Figure 7.12: 3×RRR planar parallel mechanism.

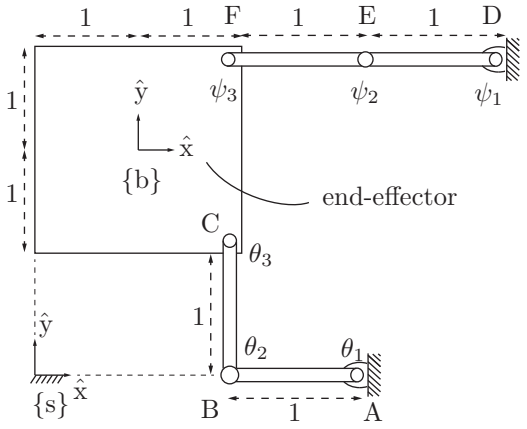

Figure 7.13: A six-bar-linkage.

Exercise 7.5 Consider the 3×PSP spatial parallel mechanism of Figure 7.14.
(a) How many degrees of freedom does this mechanism have?
(b) Let $R_{sb} = \text{Rot}(\hat{z}, \theta)\text{Rot}(\hat{y}, \phi)\text{Rot}(\hat{x}, \psi)$ be the orientation of the body frame

{b}, and let $p_{sb} = (x, y, z) \in \mathbb{R}^3$ be the vector from the {s}-frame origin to the {b}-frame origin (both R_{sb} and p_{sb} are expressed in {s}-frame coordinates). The vectors $\mathrm{a}_i, \mathrm{b}_i, \mathrm{d}_i$, $i = 1, 2, 3$, are defined as shown in the figure. Derive a set of independent kinematic constraint equations relating $(\theta, \phi, \psi, x, y, z)$ and the defined vectors.

(c) Given values for (x, y, z), is it possible to solve for the vertical prismatic joint values s_i, where $s_i = \|\mathrm{d}_i\|$ for $i = 1, 2, 3$? If so, derive an algorithm for doing so.

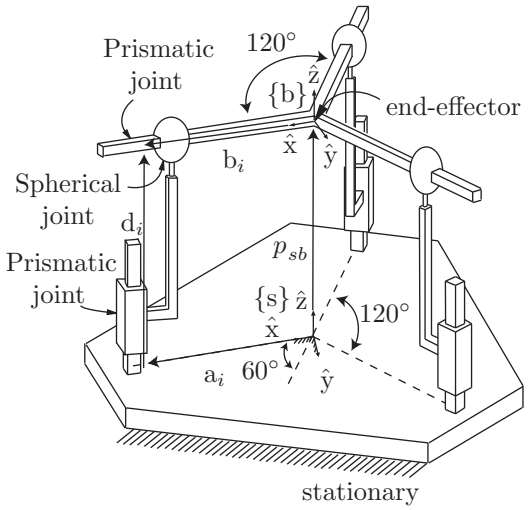

Figure 7.14: 3×PSP spatial parallel manipulator.

Exercise 7.6 The Eclipse mechanism of Figure 7.15 is a six-dof parallel mechanism whose moving platform can tilt by ±90° with respect to ground and can also rotate by 360° about the vertical axis. Assume that the six sliding joints are actuated.

(a) Derive the forward and inverse kinematics. How many forward kinematic solutions are there for general nonsingular configurations?

(b) Find and classify all singularities of this mechanism.

Exercise 7.7 For the Delta robot of Figure 7.1(b), obtain the following:

(a) the forward kinematics,

(b) the inverse kinematics,

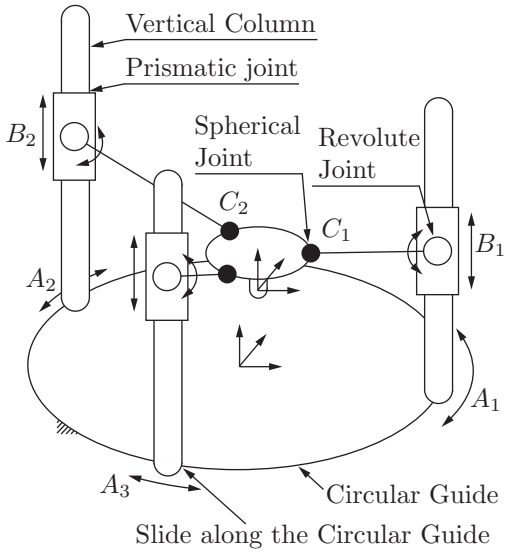

Figure 7.15: The Eclipse mechanism.

(c) the Jacobian J_a (assume that the revolute joints at the fixed base are actuated).
(d) Identify all actuator singularities of the Delta robot.

Exercise 7.8 In the 3×UPU platform of Figure 7.16, the axes of the universal joints are attached to the fixed and moving platforms in the sequence indicated, i.e., axis 1 is attached orthogonally to the fixed base, while axis 4 is attached orthogonally to the moving platform. Obtain the following:
(a) the forward kinematics,
(b) the inverse kinematics,
(c) the Jacobian J_a (assume that the revolute joints at the fixed base are actuated).
(d) Identify all actuator singularities of this robot.
(e) If you can, build a mechanical prototype and see whether the mechanism behaves as predicted by your analysis.

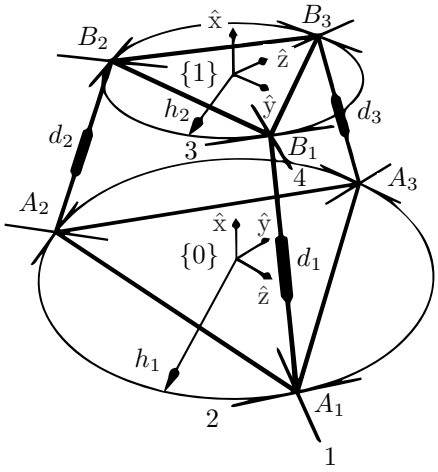

Figure 7.16: The 3×UPU mechanism.